Improved simulation of Antarctic sea ice due to the radiative effects of falling snow

To cite this article: J-L F Li *et al* 2017 *Environ. Res. Lett.* **12** 084010

View the article online for updates and enhancements.

Related content

Environmental Research Letters

LETTER

Improved simulation of Antarctic sea ice due to the radiative effects of falling snow

J-L F Li[1,6], Mark Richardson[1], Yulan Hong[4], Wei-Liang Lee[2] , Yi-Hui Wang[1], Jia-Yuh Yu[3], Eric Fetzer[1], Graeme Stephens[1] and Yinghui Liu[5]

1   Jet Propulsion Laboratory, California Institute of Technology, Pasadena, CA, United States of America
2   RCEC, Academia Sinica, Taipei, Taiwan
3   Department of Atmospheric Sciences, National Central University, Taoyuan City, Taipei, Taiwan
4   Department of Earth, Ocean and Atmospheric Science, Florida State University, Tallahassee, FL, United States of America
5   Cooperative Institute for Meteorological Satellite Studies, UW-Madison, WI, United States of America
6   Author to whom any correspondence should be addressed.

E-mail: jli@jpl.nasa.gov

Abstract

Southern Ocean sea-ice cover exerts critical control on local albedo and Antarctic precipitation, but simulated Antarctic sea-ice concentration commonly disagrees with observations. Here we show that the radiative effects of precipitating ice (falling snow) contribute substantially to this discrepancy. Many models exclude these radiative effects, so they underestimate both shortwave albedo and downward longwave radiation. Using two simulations with the climate model CESM1, we show that including falling-snow radiative effects improves the simulations relative to cloud properties from CloudSat-CALIPSO, radiation from CERES-EBAF and sea-ice concentration from passive microwave sensors. From 50–70°S, the simulated sea-ice-area bias is reduced by 2.12×10^6 km^2 (55%) in winter and by 1.17×10^6 km^2 (39%) in summer, mainly because increased wintertime longwave heating restricts sea-ice growth and so reduces summer albedo. Improved Antarctic sea-ice simulations will increase confidence in projected Antarctic sea level contributions and changes in global warming driven by long-term changes in Southern Ocean feedbacks.

1. Introduction

The Southern Ocean and Antarctica are climatically important due to Antarctic ice-sheet melt contributing to sea-level rise, changes in sea-ice cover contributing to albedo feedbacks, and the importance of oceanic heat uptake in this region for global energy balance and heat transport. The area of sea-ice in the Southern Ocean changes hugely with the seasons [van den Broeke 2004, Simmonds 2015] and is currently poorly represented in current climate models. Recent studies have shown that the Coupled Model Intercomparison Project, phase 5 (CMIP5) global climate models (GCMs) do not show an overall improvement in the simulation of Antarctic sea-ice compared to those in the older Coupled Model Intercomparison Project, phase 3 (CMIP3) [Turner *et al* 2013, 2014, Mahlstein *et al* 2013, Lefebvre and Goosse 2007, Simmonds 2015,

Zunz *et al* 2013]. We focus on the mean state here, although we note that most CMIP5 models simulated retreating Antarctic sea-ice over 1979–2005, in contrast to the observed statistically significant increase in most months [Simmonds 2015]. Some studies have shown that these changes are within the natural variability simulated by CMIP5 [Meehl *et al* 2016, Polvani and Smith 2013, Gagné *et al* 2015], and the observed increase is now less robust in many months following reductions in 2016 and 2017. We provide a further discussion on trends in supplementary information but otherwise do not address them.

Sea-ice cover strongly affects surface energy budgets through its high albedo and by restricting heat and moisture exchange between the ocean and atmosphere and simulations indicate an important role for this region in future climate change. For example, Armour *et al* [2013] found that strong

amplifying feedbacks in the Southern Ocean over centennial timescales contribute to an increase of apparent climate sensitivity with time i.e. increased global warming in response to a given forcing. If this is accurate then calculations using current observational records likely underestimate equilibrium climate response, meaning that the carbon budget for any given temperature target is smaller than inferred from these calculations. Given that this is a modelled result relying heavily on Southern Ocean changes, improved simulation of the regional sea-ice and energy budget in the present day is necessary to increase confidence.

Partial collapse of the West Antarctic ice-sheet is a major climate risk [Joughin and Alley 2011, Joughin *et al* 2014, Bamber *et al* 2009] but relevant thresholds and timescales have not been precisely identified despite extensive research on recent Antarctic mass balance [Shepherd *et al* 2012, McMillan *et al* 2014, Zwally *et al* 2015, Holland *et al* 2017]. Confounding factors include extreme storms causing large short-term mass increases [Boening *et al* 2012, Lenaerts *et al* 2016], and uncertainties in how long-term warming is expected to increase snowfall as well as melt and dynamical loss [Winkelmann *et al* 2012]. Changes in modelled precipitation over Antarctica are linked to sea-ice cover [Palerme *et al* 2016], so improved representations of sea-ice conditions in models is therefore important to help determine the credibility of projections of Antarctic changes.

Antarctica's relative isolation thanks to the strength of the Antarctic Circumpolar Current (ACC), its surrounding belt of westerlies and upwelling cool water [Armour *et al* 2016] mean that its forced response to climate change is weak relative to internal variability. The Southern Hemisphere dominates recent ocean heat storage [Stephens *et al* 2016] but otherwise this delayed Southern-Hemisphere response to forced changes makes it difficult to observationally constrain factors important for future climate change and sea-level rise. Holland *et al* [2017] shows that models simulate a two-timescale response to positive Southern Annular Mode (SAM) anomalies, with an initial increase in ice followed by an eventual sea-ice decline, further complicating the interpretation of short-term sea-ice records.

Local radiation contributes to sea-ice changes, and one challenge for GCMs is the correct radiative representation of clouds. Cloud properties in fully coupled GCMs often disagree with observations [Li *et al* 2013, Lenaerts *et al* 2017]. Here we focus on examining the radiative effects of considering precipitating ice clouds (i.e. snow) as 26 out of 40 CMIP5 GCMs do not consider these effects [Li *et al* 2012, Waliser *et al* 2009] (see supplementary table 1 available at stacks.iop.org/ERL/12/084010/mmedia).

A number of physical processes have been shown to contribute to differences in GCM representations of energy budgets and sea-ice in the Southern Ocean, including the abundance and brightness of clouds

[Trenberth and Fasullo 2010], the representation of supercooled liquid droplets [Cesana *et al* 2012, McCoy *et al* 2015, Kay *et al* 2016] and the importance of regional topography and bathymetry [Nghiem *et al* 2016]. Here we quantify the contribution of precipitating-ice radiative effects and show that it is another important factor in modelled Antarctic sea-ice biases.

A series of studies has demonstrated the importance of precipitating-ice radiative effects for explaining model biases in radiation fields that are well correlated with biases in other simulated properties such as near-surface temperatures [Li *et al* 2013, Li *et al* 2014, Li *et al* 2015, Li *et al* 2016]. We use specialized simulations where we turn on or off the precipitating-ice radiative effects and compare these with observation-based products. Here we begin by summarizing the regional importance of precipitating-ice radiative effects for reducing the model-observation discrepancy in cloud and radiation properties. We then extend this analysis to the simulation of Antarctic sea-ice and show that including these radiative effects substantially reduces the discrepancy between simulated and observed sea-ice area. Our inclusion of snow radiative effects also reduces model-observation discrepancy of Arctic sea-ice concentration, but differences in geography between the Arctic and Antarctic complicate a joint analysis. Therefore, we restrict our discussion here to Antarctic sea-ice.

2. Methods

2.1. Climate Model Simulations

As historical simulations end in 2005 and satellite sea-ice series begin in the late 1970s, we select output from 1980–2005 and for each grid-cell take the mean of the CMIP5 simulations for a given month and given property. There is little difference in the average properties between the CMIP3 and CMIP5 ensembles so we only report CMIP5 results here (supplementary figure 1). All CMIP5 models together are reported the Multi-Model Mean (CMIP5 M MM, Taylor *et al* 2012), and we separately present the mean for those models both with and without falling-snow radiative effects (CMIP5-S and CMIP5 NoS respectively, see supplementary table 1).

For our intervention 'snow radiative effects on' (S) and 'snow radiative effects off' (NoS) simulations we use the Community Earth System Model version 1 (CESM1) managed by National Center for Atmospheric Research (NCAR) and Department of Energy (DOE) which is composed of four separate models that simultaneously simulate Earth's atmosphere, ocean, land surface, and sea-ice. Model code and documentation are available from www.cesm.ucar.edu/models/cesm1.0/. The atmospheric model is the Community Atmosphere Model version 5 (CAM5), and snow in this model represents large ice crystals diagnosed from the falling ice mass flux at each model

level and time step [Morrison and Gettelman 2008, Neale *et al* 2012]. The model uses two-moment, stratiform cloud microphysics scheme described by Morrison and Gettelman (2008) which accounts for diagnosed snow mass. Snow is included in the radiation code [Gettelman *et al* 2010], using the diagnosed mass and effective radius of falling snow crystals [Morrison and Gettelman 2008]. The simulated prognostic ice and diagnostic snow are comparable against *CloudSat-CALIPSO* retrieved products [Gettelman *et al* 2010]. More detailed descriptions and related references are in supplementary information section 2.

We conduct sensitivity experiments using a fully coupled setup with two simulations over 1850–2005: one excludes the precipitating ice radiative effect (NoS); and the other includes the effect (S). Each simulation otherwise follows the CMIP5 historical protocol, including initialization from the same CESM1 C AM5 CMIP5 300 year preindustrial control (piControl) run.

The global area-weighted mean of the net radiative flux at top of atmosphere (TOA) over the full simulation is -0.17 W m^{-2} and 0.12 W m^{-2} for the NoS and S cases, respectively. The reflected SW TOA flux is -1.6 W m^{-2} for NoS and 0.6 W m^{-2} for S and the outgoing LW at TOA is 0.6 W m^{-2} for NoS and -1.9 W m^{-2} for S.

Changes in model-observation discrepancy between the S and NoS cases are determined from:

$$\Delta x = |x_{NoS} - x_{obs}| - |x_S - x_{obs}| \qquad (1)$$

where x is some property, the subscript *NoS* represents the value from the NoS simulation, *S* is from the snow simulation and *obs* denotes the observation-based value. We use this metric in figures 5(*c*) and (*f*), and it is defined such that a positive value represents a decrease in the magnitude of the model-observation discrepancy when snow-radiative effects are included.

2.2. Comparison with observation-based cloud- and radiation properties
We begin by highlighting the importance of including falling snow to cloud properties by considering biases over Antarctica and the Southern Oceans in the CMIP5 NoS ensemble average. We first compare modelled cloud properties with those determined over 2007–2010 from CloudSat-CALIPSO measurements. CloudSat and CALIPSO are satellites in the Afternoon-Train (A-train) constellation that fly along the same reference ground track on a Sun-synchronous orbit with an ascending (northward) local equatorial crossing time near 13:36. CALIPSO and CloudSat are separated by less than a minute, allowing reliable collocation between the CALIPSO-mounted CALIOP LIDAR and the CloudSat-mounted Cloud-Profiling Radar. We use the CALIPSO-CloudSat 2 C-ICE product [Deng *et al* 2010, 2013] over the region

40–82 °S where the poleward edge is limited by the satellites' orbit. Cloud ice water path (CIWP) is identified using the FLAG method [Li *et al* 2012] which separates cloud-only (floating or suspended cloud ice) and precipitating + convective clouds, and we use both in our comparison. Because of negligible sampling biases of cloud water, cloud formation etc [Li *et al* 2012, Guan *et al* 2013], the uncertainties related to the diurnal cycle and sampling issues are not specifically considered in the model-observation comparisons in this study.

For an observation-based estimate of surface radiation we use the satellite-based Clouds and the Earth's Radiant Energy System-Energy Balanced and Filled (CERES-EBAF) Surface products over 2000–2010, which are widely used and have been validated with surface measurements, with a monthly-grid-mean uncertainty of $\pm$ 10 W m^{-2} for shortwave and ± 14 W m^{-2} for longwave [Kato *et al* 2011, Kato *et al* 2012, 2013]. We select the same 40–82 °S region and use each of the radiative energy-budget components: longwave up and down plus shortwave up and down.
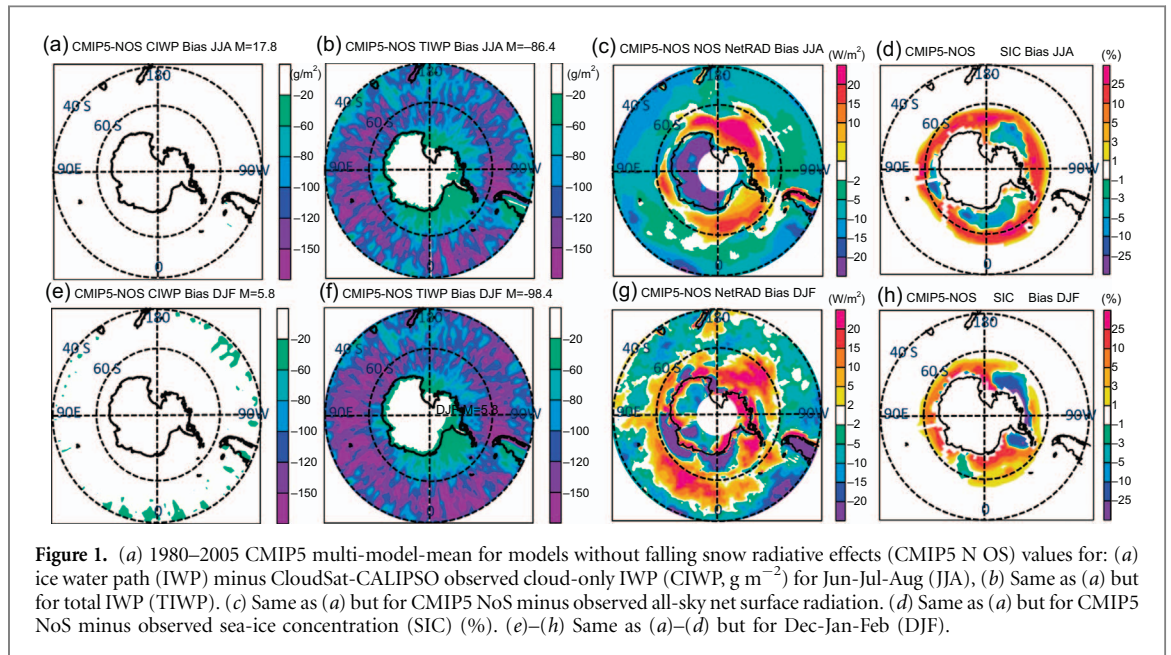
2.3. Comparison with observation-based sea-ice concentration
We take gridded monthly-averaged sea-ice concentration data from the National Snow and Ice Data Center (NSIDC) over 1980–2005 derived from the NASA Team Algorithm [Cavalieri *et al* 2012, 1999]. These are based on measurements from passive microwave sensors beginning with the Scanning Multichannel Microwave Radiometer (SMMR) aboard the Nimbus-7 satellite and proceeding with the Special Sensor Microwave/Imager (SSMI) instruments aboard the Defense Meteorological Satellite Program (DMSP) F8, F11, F13, and F17 platforms. The data's native resolution of 25 km is remapped onto a 1°×1° latitude-longitude grid and we use data from 50–70°S, excluding areas closer to Antarctica to avoid discrepancies in mapping of the Antarctic coast and its ice shelves. 82% of the magnitude of the annual cycle of sea-ice area is captured within this area, so our results apply to the majority of the sea-ice area.

3. Results

3.1. CMIP5 Biases in cloud- and radiation properties
Figure 1 shows that the CMIP5 NoS models have little bias in a like-with-like comparison with CloudSat-CALIPSO Cloud Ice-Water Path (CIWP; cloud ice only) in both Austral winter (figure 1(*a*): June-July-August, JJA) and Austral summer (figure 1(*e*): December-January-February, DJF). However, the CMIP5 NoS substantially underestimates total IWP (TIWP) over and near Antarctica once precipitating clouds are included (figure 1(*b*): JJA; figure 1(*f*): DJF). This contributes to a multi-model mean (MMM) bias

Figure 1. (*a*) 1980–2005 CMIP5 multi-model-mean for models without falling snow radiative effects (CMIP5 N OS) values for: (*a*) ice water path (IWP) minus CloudSat-CALIPSO observed cloud-only IWP (CIWP, g m^{-2}) for Jun-Jul-Aug (JJA), (*b*) Same as (*a*) but for total IWP (TIWP). (*c*) Same as (*a*) but for CMIP5 NoS minus observed all-sky net surface radiation. (*d*) Same as (*a*) but for CMIP5 NoS minus observed sea-ice concentration (SIC) (%). (*e*)–(*h*) Same as (*a*)–(*d*) but for Dec-Jan-Feb (DJF).

in total ice water path of -90.7 g m^{-2} with relative bias of -72% averaged over the region 40–82°S, relative to the CloudSat-CALIPSO 2 C-ICE product [Deng *et al* 2010, 2013]. The spatial patterns and magnitudes of TIWP biases between CMIP3 and CMIP5 are similar with an absolute bias larger than 110 g m^{-2} over the Southern Ocean, implying a zeroth-order deficiency embedded in both NoS CMIP3 and NoS CMIP5 GCMs (see supplementary figure 1). Figure 1 also shows cloud and net surface radiation biases between CMIP5 NoS and CERES-EBAF (figure 1(*c*): JJA; figure 1(*g*): DJF) and sea-ice concentration biases (figure 1(*d*): JJA; figure 1(*h*): DJF) between CMIP5 NoS and NSIDC.

Given the correlation between patterns of bias in TIWP, surface fluxes and sea-ice concentration, we propose a causal link as follows: models without falling-snow radiative effects underestimate TIWP, reducing surface downward longwave and increasing surface downward shortwave fluxes, which drive changes in sea-ice concentration (see supplementary figures 2 and 3 for the radiation budget split into its components). We support our hypothesis using specialized simulations to isolate and quantify the contribution of falling-snow radiative effects. These specialized simulations are necessary as the comparison in figure 1 includes all potential biases in simulated physical processes between CMIP5 NoS and the real-world state.

3.2. Falling-snow radiative effects and the annual cycle of modelled energy budgets and sea-ice concentration

For our quantification of the precipitating-ice radiative effects, we present results from our CESM1 simulations both with (S) and without (NoS) the radiative effects of falling snow. Figure 2 shows the model minus observed monthly values of surface radiation budget

components and sea-ice concentration, presented for two different latitude bands. This illustrates that the S simulation is consistently closer than the NoS simulation to the observed energy-budget components (figures 2(*a*), (*b*), (*d*) and (*e*) and sea-ice concentration (figures 2(*c*) and (*f*), CMIP5 M MM also shown). The largest remaining bias in the S simulations is in shortwave fluxes during austral summer, which may be related to other cloud-simulation biases such as underestimated supercooled liquid fraction in mixed-phase clouds [Tan *et al* 2016, Kay *et al* 2016] and large-scale atmospheric conditions [Simmonds 2015, Holland *et al* 2017]. Snow radiative effects reduce the size of the JJA longwave bias from 58–70°S relative to CERES-EBAF, from -30 W m^{-2} down to -10 W m^{-2} (figure 2(*d*), and the DJF shortwave bias over the same region from approximately $+55$ W m^{-2} to $+35$ W m^{-2}. We do not present a formal uncertainty estimate in these fluxes as there is a lack of CERES validation over this region. However, the reported monthly zonal mean uncertainty over oceans for the CERES data are ± 10 W m^{-2} in downward LW and SW [Kato *et al* 2012]. Our averaging over 10 year s would favor a smaller error, but the large uncertainties associated with surface albedo would favor a larger value. Taking the reported ± 10 W m^{-2} as an approximation of the error, the radiative effects of falling snow are similar in size to the observational error, and the NoS simulations are indeed in disagreement with the CERES-EBAF data over much of the year. Of the changes we see, improved model representation of downwelling long-wave radiation restricts winter sea-ice growth leading to a decrease of 2.11×10^6 km^2 in the September peak sea-ice area, whose lower level is maintained by increased shortwave absorption during the summer. This substantially reduces the bias relative to observations.
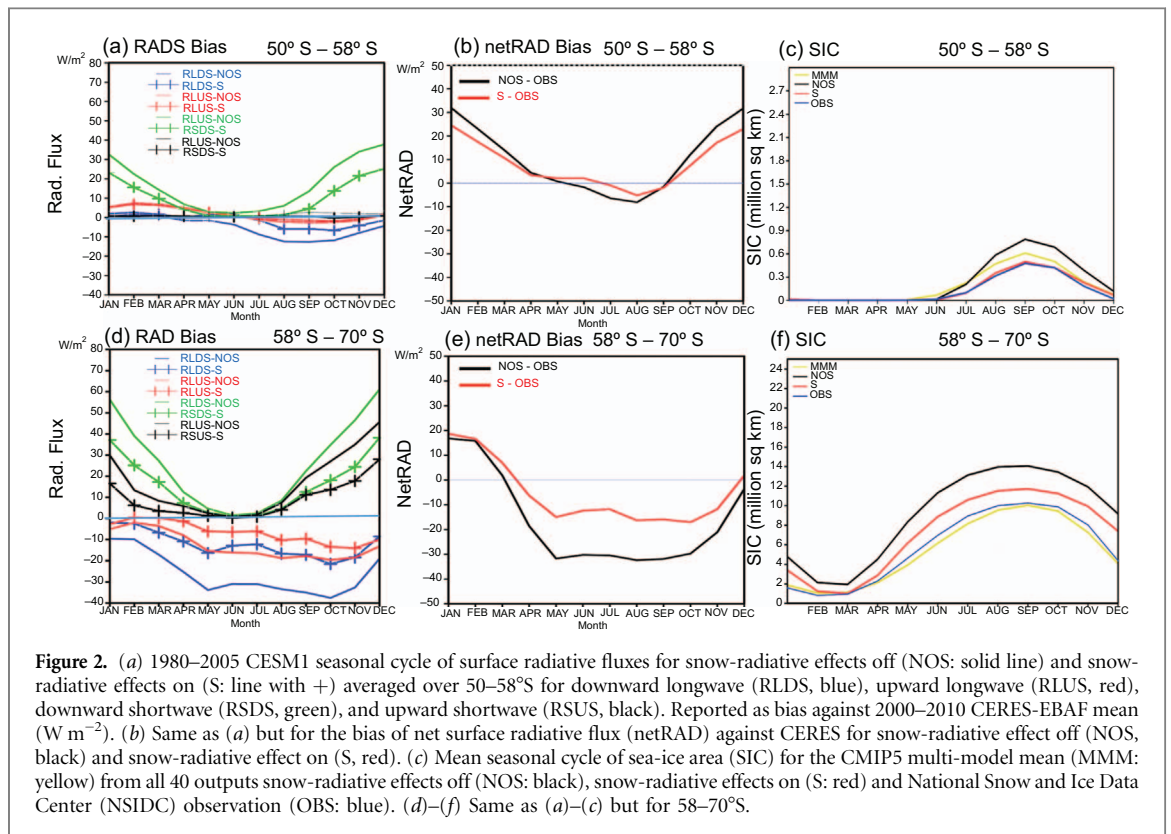
Figure 2. (*a*) 1980–2005 CESM1 seasonal cycle of surface radiative fluxes for snow-radiative effects off (NOS: solid line) and snow-radiative effects on (S: line with +) averaged over 50–58°S for downward longwave (RLDS, blue), upward longwave (RLUS, red), downward shortwave (RSDS, green), and upward shortwave (RSUS, black). Reported as bias against 2000–2010 CERES-EBAF mean (W m^{-2}). (*b*) Same as (*a*) but for the bias of net surface radiative flux (netRAD) against CERES for snow-radiative effect off (NOS, black) and snow-radiative effect on (S, red). (*c*) Mean seasonal cycle of sea-ice area (SIC) for the CMIP5 multi-model mean (MMM: yellow) from all 40 outputs snow-radiative effects off (NOS: black), snow-radiative effects on (S: red) and National Snow and Ice Data Center (NSIDC) observation (OBS: blue). (*d*)–(*f*) Same as (*a*)–(*c*) but for 58–70°S.

Figure 3 shows a spatial anti-correlation in the NoS minus S (NoS-S) change in JJA. When snow radiative effects are excluded, the underestimated IWP results in increased net surface shortwave flux (RSDS-RSUS: figures 3(*a*), (*b*)) and decreased surface downward longwave flux (RLDS: figure 3(*c*)). Longwave dominates in austral winter, meaning smaller net radiation (figure 3(*e*)), cooler surface temperature (see supplementary figures 4 and 5) and increased sea-ice concentration (figure 3(*f*)).
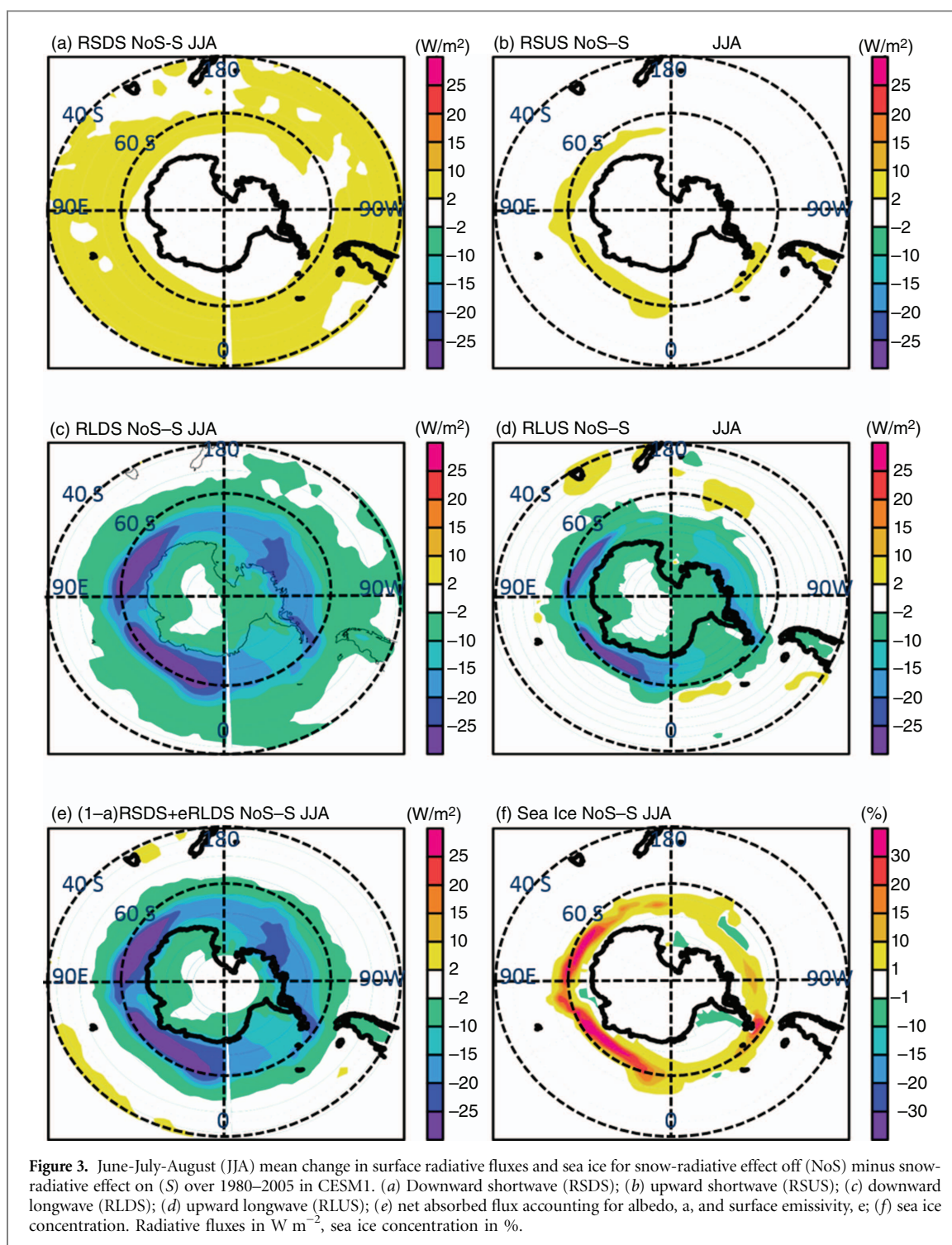
Figure 4 shows that during austral summer the situation is more complex. In some regions, such as off the coast of Dronning-Maud land, there is a net decrease in downward radiation (figure 4(*e*)) along with a net decrease in sea-ice concentration (figure 4(*f*)). This is counterintuitive, but can be understood from the seasonal cycles in figure 2. In these regions, the increased winter longwave heating restricts sea-ice growth and leads to a reduced surface albedo. Although less sunlight reaches the surface due to atmospheric reflection by falling snow, the surface is darker due to reduced winter sea-ice growth caused by increased wintertime longwave heating. This increases absorption by enough to offset the reduction in downward shortwave radiation at the surface, helping to prevent summertime sea-ice growth in these regions.

We consider these effects in more detail and determine their robustness in figure 5, which maps changes in the bias in sea-ice concentration during JJA and DJF for the S and NoS simulations and the relative difference in bias from equation (1). In this case, positive means a reduction in bias magnitude. The

inclusion of snow radiative effects leads to a widespread decrease in sea-ice concentration that brings the simulated sea-ice case closer to observations in most regions, with the exception of a band centered near 45°E in JJA.

From 50–70 °S the NoS simulations of sea-ice area have a relative bias of 3.01×10^6 km^2 in DJF and 3.88×10^6 km^2 in JJA, which is reduced in the S simulations to 1.84×10^6 km^2 (by 39%) in DJF and 1.75×10^6 km^2 (by 55%) in JJA. The greatest absolute change is in March-April-May (MAM) where the discrepancy is reduced by 65%. September-October-November (SON) shows a reduction of 54%. Using t-tests applied to the monthly simulated time series, the differences are statistically robust with, for example, sea-ice concentration changes significant at $p < 0.01$ over much of the Southern Ocean (supplementary figures 6 and 7). The surface radiation budget and surface or near-surface temperature biases are also reduced in most regions (supplementary figures 8 and 9).

Figure 6 shows mean SIC seasonal cycles from a range of sources. Figures 6 (*a*), (*d*) and (*g*) show the 40 m ember full CMIP5 ensemble along with the multi-model mean (MMM) and standard deviation. Figures 6(*b*), (*e*) and (*h*) show where the observations and CESM-1 S and NoS simulations fall within the CMIP5 distribution. Figures 6(*c*), (*f*) and (*i*) show the CMIP5 MMM versus observations along with the mean for CMIP5 NoS models ($N = 14$) and CMIP5-S models ($N = 26$). The CMIP5 mean annual cycle is similar to observations, with slight underestimates in maximum extent, as reported elsewhere [Zunz *et al* 2013, Lenaerts *et al* 2016, Boucher *et al* 2013,

Figure 3. June-July-August (JJA) mean change in surface radiative fluxes and sea ice for snow-radiative effect off (NoS) minus snow-radiative effect on (S) over 1980–2005 in CESM1. (*a*) Downward shortwave (RSDS); (*b*) upward shortwave (RSUS); (*c*) downward longwave (RLDS); (*d*) upward longwave (RLUS); (*e*) net absorbed flux accounting for albedo, a, and surface emissivity, e; (*f*) sea ice concentration. Radiative fluxes in W m^{-2}, sea ice concentration in %.

IPCC 2013]. Consistent with our CESM1 results, the CMIP5-S models show less sea-ice than the CMIP5 NoS models. The CMIP5-S underestimate of sea-ice extent indicates that other aspects of the model design likely overcompensate for the inclusion of snow radiative effects.

4. Discussion and conclusions

We have investigated CMIP5 biases relative to observations over the Antarctic sea-ice region and

attributed some of these biases to the exclusion of falling-ice radiative effects in most models. We showed that for the 26 out of 40 CMIP5 models that do not simulate precipitating ice radiative effects, the multi-model mean cloud ice water path agrees well with the non-precipitating cloud ice water path identified from CloudSat-CALIPSO observations. However, there is a substantial bias in total cloud ice-water path due to the exclusion of model falling-snow radiative effects. Total ice-water path is underestimated by about 100 g m^{-2} over much of the Southern Ocean, contributing to an underestimate in downward longwave radiation and
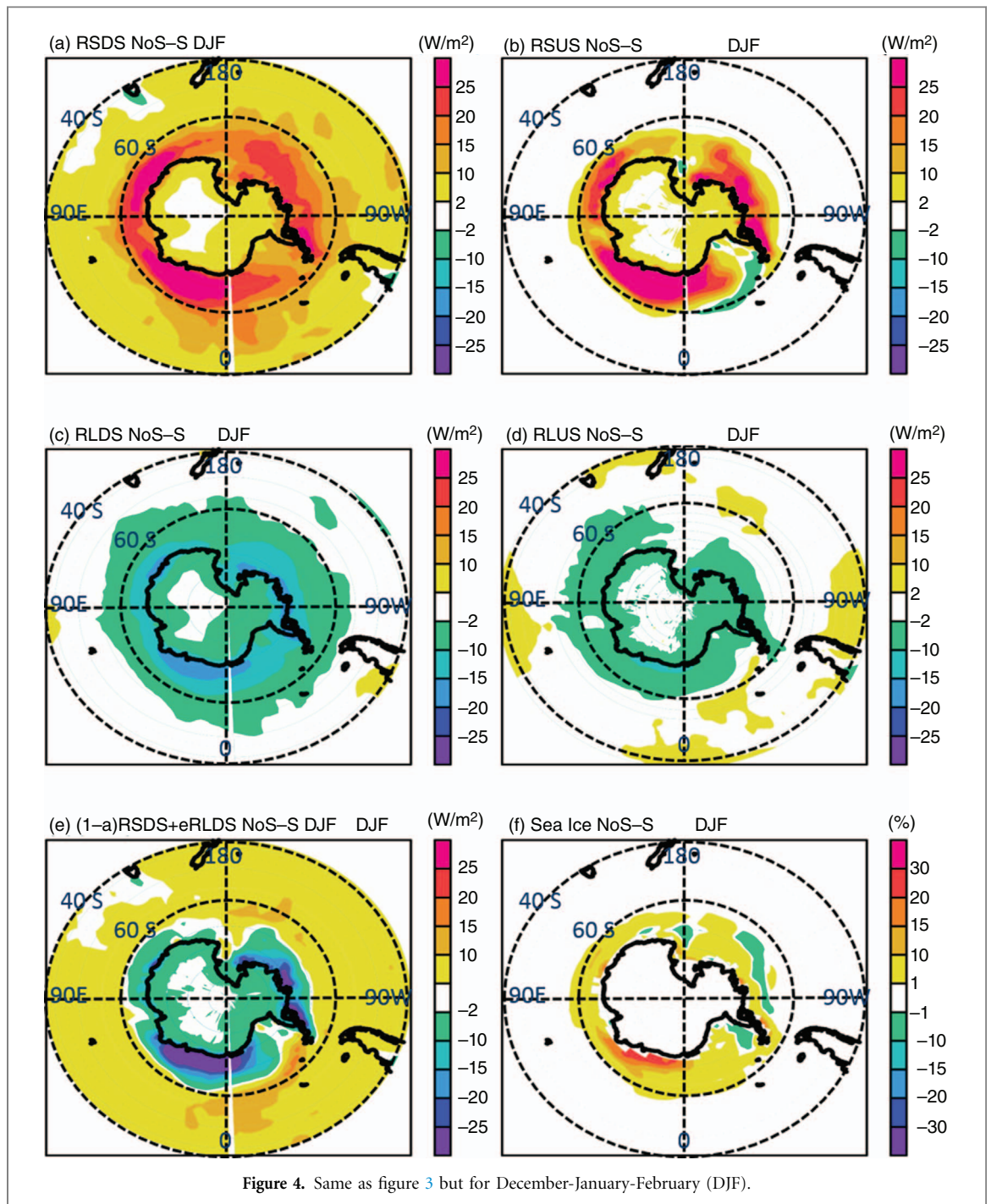
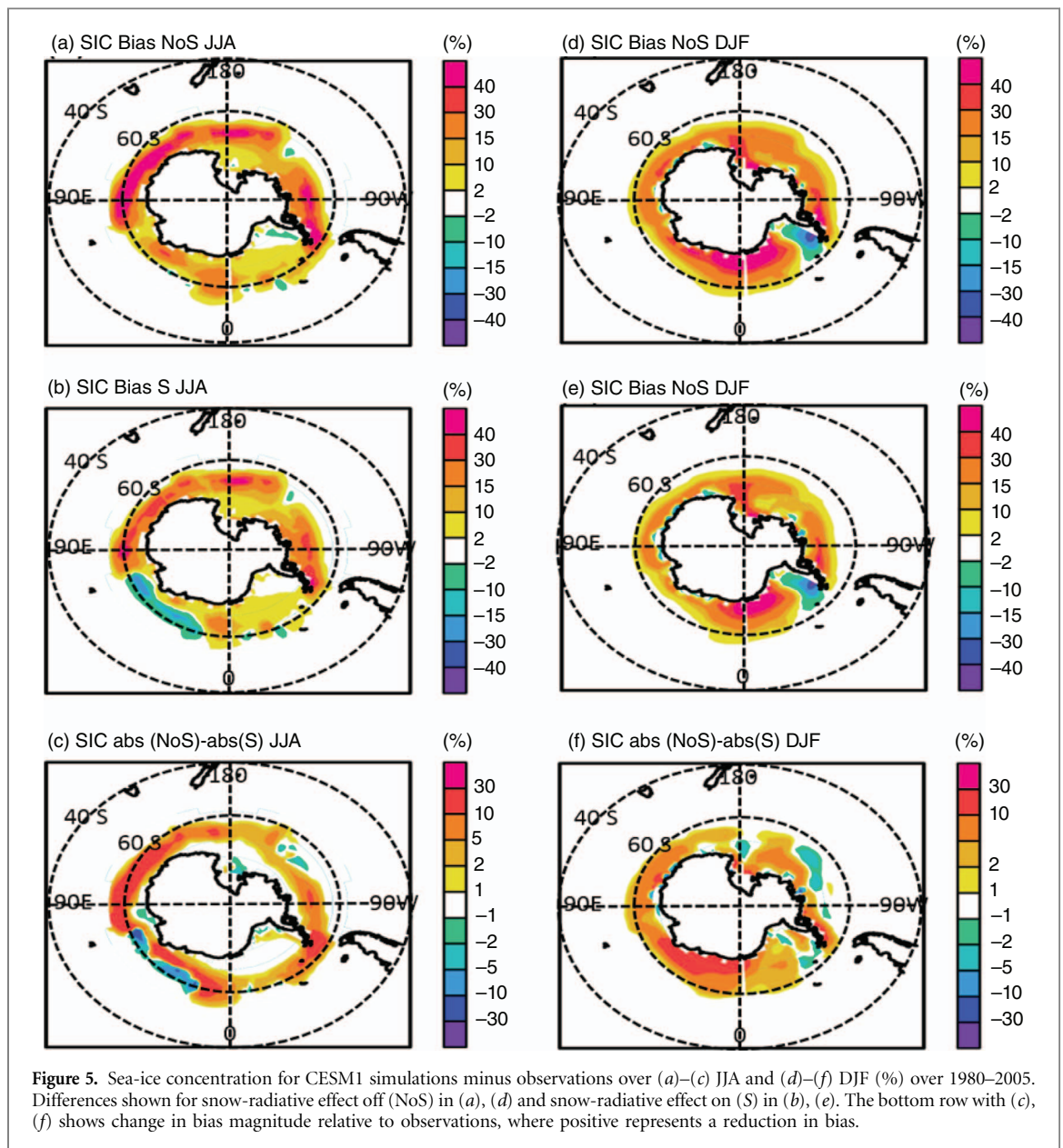**Figure 4.** Same as figure 3 but for December-January-February (DJF).

an overestimate in downward shortwave radiation at the surface.

Through controlled simulations using the CESM1 in which we activated or deactivated the snow radiative effects, we demonstrated that this radiation reduces the model-observed discrepancy in sea-ice area at 50–70°S by 39–66%, depending on the season. The geographical pattern of SIC and radiation fields changes largely matches the CMIP5-S multi-model mean bias. From inspection of the annual cycle, it appears that the improvements in representation of sea-ice are driven by an increase in downward longwave radiation due to increased ice-water path with inclusion of precipitating ice during winter (JJA). This restricts the growth of sea ice, leading to a lower

mean sea-ice area of 2.11×10^6 km^2 in 1980–2005 during September, the month of peak sea-ice cover. During austral summer, increased reflection by cloud ice reduces the shortwave radiation arriving at the surface, in some regions by an amount greater than the increased downwelling longwave due to this ice. However, this does not increase sea-ice concentration because during the previous winter, cloud-ice radiative effects restricted sea-ice growth and reduced surface albedo. This memory effect from the previous winter more than offsets the reduced amount of sunlight reaching the surface during summer.

Falling-snow radiative effects are therefore important for simulating radiative balance and sea-ice concentration over the Southern Ocean and this has

Figure 5. Sea-ice concentration for CESM1 simulations minus observations over (*a*)–(*c*) JJA and (*d*)–(*f*) DJF (%) over 1980–2005. Differences shown for snow-radiative effect off (NoS) in (*a*), (*d*) and snow-radiative effect on (S) in (*b*), (*e*). The bottom row with (*c*), (*f*) shows change in bias magnitude relative to observations, where positive represents a reduction in bias.
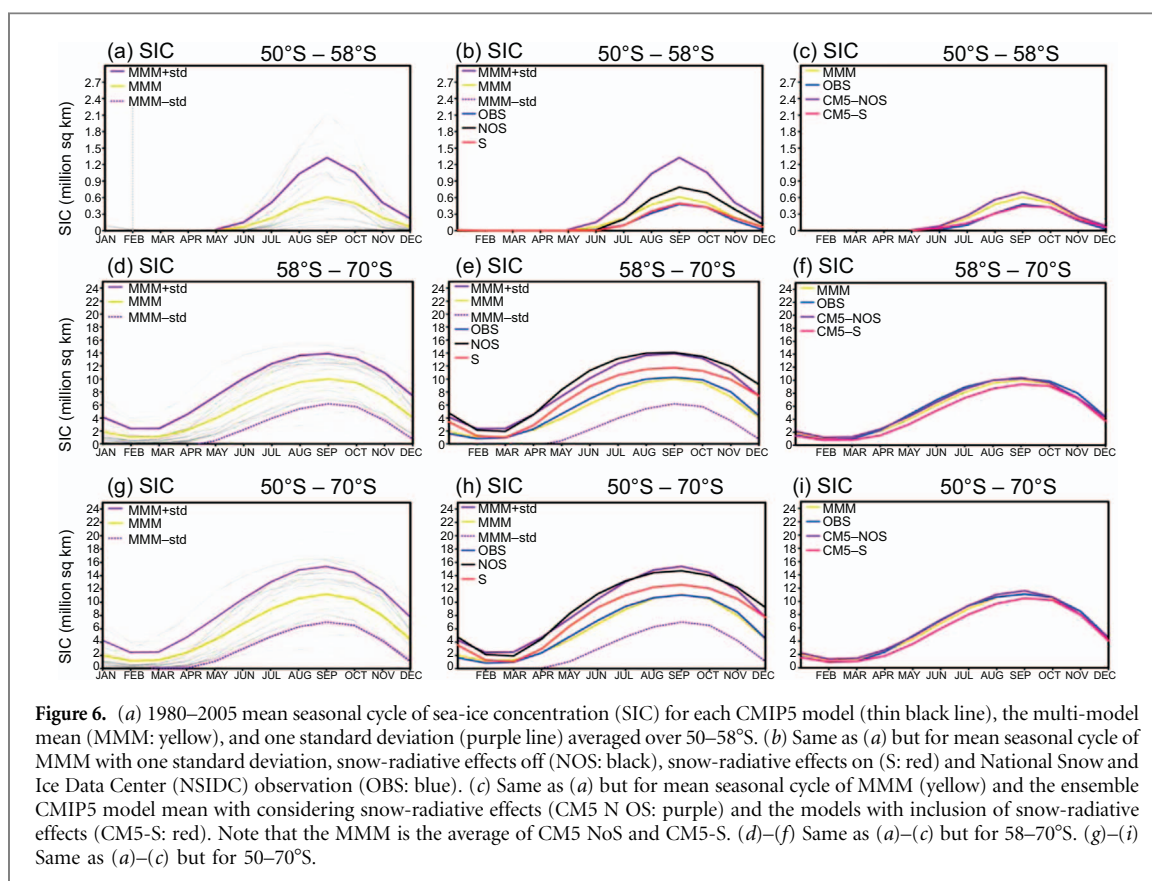
not been previously quantified. Studies have shown that multiple factors contribute to model Southern-Ocean sea-ice biases, and we only argue that the evidence shows that radiative effects of falling snow are an additional candidate, but one with substantial effects on simulated energy budgets and sea ice. Such a physics-based improvement, if applied across models, would increase confidence in projections of regional changes affecting climate feedbacks. In addition, better representation of sea-ice should improve water flux and therefore simulated Antarctic bottom water (AABW) and Southern Ocean temperature profiles, which are currently poorly simulated (e.g. Rhein *et al* 2013, IPCC AR5 report). We do not argue that precipitating-ice radiative effects are the only domi-nant factor in model biases related to sea ice. However, given the reduction in model-observation discrepancy of 39–66% when including falling-snow radiative effects, we conclude that the exclusion of precipitating snow particles is a critical shortcoming of 26 of the 40

state-of-the-art GCMs used to project the future state of Antarctic sea ice. Given that falling-snow radiative effects are already included in some models, this is an opportunity to address an easily understood, physi-cally based deficiency that may introduce notable biases in climate simulations. Including falling-snow radiative effects is an obvious opportunity for improvement across the majority of climate models used in the widely referenced reports of the Intergovernmental Panel on Climate Change (IPCC).

Acknowledgments

Figure 6. (*a*) 1980–2005 mean seasonal cycle of sea-ice concentration (SIC) for each CMIP5 model (thin black line), the multi-model mean (MMM: yellow), and one standard deviation (purple line) averaged over 50–58°S. (*b*) Same as (*a*) but for mean seasonal cycle of MMM with one standard deviation, snow-radiative effects off (NOS: black), snow-radiative effects on (S: red) and National Snow and Ice Data Center (NSIDC) observation (OBS: blue). (*c*) Same as (*a*) but for mean seasonal cycle of MMM (yellow) and the ensemble CMIP5 model mean with considering snow-radiative effects (CM5 N OS: purple) and the models with inclusion of snow-radiative effects (CM5-S: red). Note that the MMM is the average of CM5 NoS and CM5-S. (*d*)–(*f*) Same as (*a*)–(*c*) but for 58–70°S. (*g*)–(*i*) Same as (*a*)–(*c*) but for 50–70°S.

the NASA Making Earth System Data Records for Use in Research Environments (MEaSUREs) programs.

The most up-to-date Radiative Longwave Downward flux at Surface (RLDS) and Radiative Shortwave Downward flux at Surface (RSDS) are available from EBAF-Surface and ISCCP derived products. This surface flux radiation product is constrained by TOA CERES-derived flux with Energy Balanced and Filled (EBAF) adjustments [39–41]. The data used in this study is the monthly mean product, collected from January 2000 to December 2010. The CERES data can be found at http://ceres.larc.nasa.gov/order_data.php.

The land surface temperature is monthly composite and average of the MODIS Level-3 LST product (MOD11C3) at 0.05 degree grid resolution (2002 to 2012). Further details regarding the MODIS land product validation for the LST/E products is available from the following URL: http://landval.gsfc.nasa.gov/ProductStatus.php?ProductID=MOD11. The surface air temperature climatology used in this study is based on the period of 1961–1990 from HADCRUT2V data. The data can be accessed at www.esrl.noaa.gov/psd/data/gridded/data.hadcru3.html. The monthly mean UDel land-only SAT data span from 1900 to 2010 can be accessed at http://climate.geog.udel.edu/~climate/html_pages/download.html and references can be found at the http://climate.geog.udel.edu/~climate/.

For sea-ice observations, we utilize sea-ice concentration from the National Snow and Ice Data Center (NSIDC), where it provides the longest sea-ice

record [Cavalieri *et al* 2012]. Here, we use the monthly mean sea-ice concentration data from 1978 to 2014 derived from NASA Team algorithm. The monthly mean sea-ice concentration data is available at 25 km Polar Stereographic Projections in both north and south polar regions (https://nsidc.org/data/seaice/data_summaries.html). These data are then re-gridded to global 1° longitude by 1° latitude.

The filtered cloud ice, ice water path and cloud fraction data span from 2007 to 2010 are available by email request (jli@jpl.nasa.gov).

ORCID iDS

Wei-Liang Lee ⓘ https://orcid.org/0000-0003-1419-315X

References

Armour K C, Bitz C M and Roe G H 2013 Time-varying climate sensitivity from regional feedbacks *J. Clim.* **26** 4518–34

Armour K C, Marshall J, Scott J R, Donohoe A and Newsom E R 2016 Southern Ocean warming delayed by circumpolar upwelling and equatorward transport *Nat. Geosci.* **9** 549–54

Bamber J L, Riva R E M, Vermeersen B L A and LeBrocq A M 2009 Reassessment of the potential sea-level rise from a collapse of the West Antarctic ice-sheet *Science* **324** 901–3

Boening C, Lebsock M, Landerer F and Stephens G 2012 Snowfall-driven mass change on the East Antarctic ice-sheet *Geophys. Res. Lett.* **39** L21501

Boucher O *et al* 2013 *Clouds and Aerosols. Climate Change 2013: The Physical Science Basis. Contribution of Working Group I to the Fifth Assessment Report of the Intergovernmental Panel on Climate Change*

Cavalieri D J, Parkinson C L, Gloersen P, Comiso J C and Zwally H J 1999 Deriving long-term time series of sea-ice cover from satellite passive-microwave multisensor data sets *J. Geophys. Res.* **104** PP-15, 803-15, 814

Cavalieri D J, Parkinson C L, Digirolamo N and Ivanoff A 2012 Intersensor calibration between F13 SSMI and F17 SSMIS for global sea-ice data records *IEEE Geosci. Remote Sens. Lett.* **9** 233–6

Cesana G, Kay J E, Chepfer H, English J M and de Boer G 2012 Ubiquitous low-level liquid-containing Arctic clouds: new observations and climate model constraints from CALIPSO-GOCCP *Geophys. Res. Lett.* **39** L20804

Deng M, Mace G G, Wang Z and Okamoto H 2010 Tropical composition, cloud and climate coupling experiment validation for cirrus cloud profiling retrieval using CloudSat radar and CALIPSO lidar *J. Geophys. Res.* **115** D00J15

Deng M, Mace G G, Wang Z and Lawson R P 2013 Evaluation of several a-train ice cloud retrieval products with *in situ* measurements collected during the SPARTICUS campaign *J. Appl. Meteorol. Climatol.* **52** 1014–30

Gagné M-E, Gillet N P and Fyfe J C 2015 Observed and simulated changes in Antarctic sea ice extent over the past 50 years *Geophys. Res. Lett.* **42** 2014GL062

Gettelman A, Liu X, Ghan S J, Morrison H, Park S, Conley A J, Klein S A, Boyle J, Mitchell D L and Li J-L F 2010 Global simulations of ice nucleation and ice supersaturation with an improved cloud scheme in the community atmosphere model *J. Geophys. Res.* **115** D18216

Guan B, Waliser D E, Li J-L F and da Silva A 2013 Evaluating the impact of orbital sampling on satellite-climate model comparisons *J. Geophys. Res. Atmos.* **118** 355–69

Holland M M, Landrum L, Kostov Y and Marshall J 2017 Sensitivity of Antarctic sea-ice to the Southern annular mode in coupled climate models *Clim. Dyn.* (https://doi. org/10.1007/s00382-016-3424-9)

IPCC 2013 *Climate Change 2013: The Physical Science Basis Contribution of Working Group I to the Fifth Assessment Report of the Intergovernmental Panel on Climate Change* ed T F Stocker, D Qin, G K Plattner, M Tignor, S K Allen, J Boschung, A Nauels, Y Xia, V Bex and P M Midgley (Cambridge: Cambridge University Press) pp 1535 (https:// doi.org/10.1017/CBO9781107415324)

Joughin I and Alley R B 2011 Stability of the West Antarctic ice sheet in a warming world *Nat. Geosci.* **4** 506–13

Joughin I, Smith B E and Medley B 2014 Marine ice sheet collapse potentially under way for the thwaites Glacier Basin, West Antarctica *Science* **344** 735–8

Kato S *et al* 2011 Improvements of top-of-atmosphere and surface irradiance computations with CALIPSO-, CloudSat-, and MODIS-derived cloud and aerosol properties *J. Geophys. Res. Atmos.* **116** 1–21

Kato S, Loeb N G, Rutan D A, Rose F G, Sun-Mack S, Miller W F and Chen Y 2012 Uncertainty estimate of surface irradiances computed with MODIS-, CALIPSO-, and cloudSat-derived cloud and aerosol properties *Surv. Geophys.* **33** 395–412

Kato S, Loeb N G, Rose F G, Doelling D R, Rutan D A, Caldwell T E, Yu L and Weller R A 2013 Surface irradiances consistent with CERES-derived top-of-atmosphere shortwave and longwave irradiances *J. Clim.* **26** 2719–40

Kay Jennifer E, Wall C, Yettella V, Medeiros B, Hannay C, Caldwell P and Bitz C 2016 Global climate impacts of fixing the Southern Ocean Shortwave radiation bias in the community earth system model (CESM) *J. Clim. Am. Meteor. Soci.* **29** 4617–36

Lefebvre W and Goosse H 2007 Analysis of the projected regional sea-ice changes in the Southern Ocean during the twenty-first century *Clim. Dyn.* **30** 59–76

Lenaerts J T M, Vizcaino M, Fyke J, van Kampenhout L and van den Broeke M R 2016 Present-day and future Antarctic ice sheet climate and surface mass balance in the community earth system model *Clim. Dyn.* **47** 1367–81

Lenaerts J T M, Van Tricht K, Lhermitte S and L'Ecuyer T S 2017 Polar clouds and radiation in satellite observations, reanalyses, and climate models *Geophys. Res. Lett.* **44** 3355–64

Li J-L F *et al* 2012 An observationally based evaluation of cloud ice water in CMIP3 and CMIP5 GCMs and contemporary reanalyses using contemporary satellite data *J. Geophys. Res. Atmos.* **117** D16105

Li J-L F *et al* 2013 Characterizing and understanding radiation budget biases in CMIP3/CMIP5 GCMs, contemporary GCM, and reanalysis *J. Geophys. Res. Atmos.* **118** 8166–84

Li J-L F *et al* 2014 Cloud-precipitation-radiation-dynamics interaction in global climate models: a snow and radiation interaction sensitivity experiment *J. Geophys. Res. Atmos.* **119** 3809–24

Li J-L F *et al* 2015 The impacts of cloud snow radiative effects on Pacific Ocean surface heat fluxes, surface wind stress, and ocean temperatures in coupled GCM simulations *J. Geophys. Res. Atmos.* **120** 2242–60

Li J-L F *et al* 2016 The impacts of precipitating hydrometeors radiative effects on land surface temperature in contemporary GCMs using satellite observations *J. Geophys. Res. Atmos.* **121** 67–79

Mahlstein I, Gent P R and Solomon S 2013 Historical Antarctic mean sea-ice area, sea-ice trends, and winds in CMIP5 simulations *J. Geophys. Res. Atmos.* **118** 5105–10

McCoy D T, Hartmann D L, Zelinka M D, Ceppi P and Grosvenor D P 2015 Mixed-phase cloud physics and Southern Ocean cloud feedback in climate models *J. Geophys. Res. Atmos.* **120** 9539–54

McMillan M *et al* 2014 Increased ice losses from Antarctica detected by CryoSat-2 *Geophys. Res. Lett.* **41** 3899–905

Meehl G A, Arblaster J M, Bitz C M, Chung C T Y and Teng H 2016 Antarctic sea-ice expansion between 2000 and 2014 driven by tropical Pacific decadal climate variability *Nat. Geosci.* **9** 590–5

Morrison H and Gettelman A 2008 A new two-moment bulk stratiform cloud microphysics scheme in the NCAR Community Atmosphere Model (CAM3), part I: description and numerical tests *J. Clim.* **21** 3642–59

Nghiem S V, Rigor I G, Clemente-Colón P, Neumann G and Li P P 2016 Geophysical constraints on the Antarctic sea-ice cover *Remote Sens. Environ.* **181** 281–92

Neale R B 2012 *Description of the NCAR Community Atmosphere Model:CAM 5.0, Tech. Rep. NCAR/TN-486+STR* (Boulder, CO: National Center for Atmospheric Research)

Palerme C, Genthon C and Claud C 2017 Evaluation of current and projected Antarctic precipitation in CMIP5 models *Clim. Dyn.* **48** 225

Polvani L M and Smith K L 2013 Can natural variability explain observed Antarctic sea ice trends? New modeling evidence from CMIP5 *Geophys. Res. Lett.* **40** 3195–9

Rhein M *et al* 2013 Observations: ocean *Climate Change 2013: The Physical Science Basis* (Cambridge: Cambridge University Press) p 1535 (https://doi.org/10.1017/CBO9781107415324)

Simmonds I 2015 Comparing and contrasting the behaviour of Arctic and Antarctic sea-ice over the 35 year period 1979–2013 *Ann. Glaciol* **56** 18–28

Shepherd A *et al* 2012 A reconciled estimate of ice-sheet mass balance *Science* **338** 1183–9

Stephens G L *et al* 2016 The curious nature of the hemispheric symmetry of the earth's water and energy balances *Curr. Clim. Change Rep.* **2** 135–47

Tan I, Storelvmo T and Zelinka M D 2016 Observational constraints on mixed-phase clouds imply higher climate sensitivity *Science* **352** 224–7

Taylor K E, Stouffer R J and Meehl G A 2012 An overview of CMIP5 and the experiment design *Bull. Am. Meteorol. Soc.* **93** 485–98

Trenberth K E and Fasullo J T 2010 Simulation of present-day and twenty-first-century energy budgets of the Southern Oceans *J. Clim.* **23** 440–54

Turner J, Bracegirdle T J, Phillips T, Marshall G J and Hosking J S 2013 An initial assessment of Antarctic sea-ice extent in the CMIP5 models *J. Clim.* **26** 1473–84

Turner J, Hosking J S, Bracegirdle T J, Marshall G J and Phillips T 2014 Recent changes in Antarctic sea ice *Philos. Trans. R. Soc. A Math. Phys. Eng. Sci.* **373** 20140163

van den Broeke M R 2004 On the role of Antarctica as heat sink for the global atmosphere *J. Phys. IV* **121** 115–24

Waliser D E *et al* 2009 Cloud ice: a climate model challenge with signs and expectations of progress *J. Geophys. Res.* **114** D00A21

Winkelmann R, Levermann A, Martin M A and Frieler K 2012 Increased future ice discharge from Antarctica owing to higher snowfall *Nature* **492** 239–42

Zunz V, Goosse H and Massonnet. F 2013 How does internal variability influence the ability of CMIP5 models to reproduce the recent trend in southern ocean sea-ice extent *The Cryosphere* **7** 451–68

Zwally H J *et al* 2015 Mass gains of the Antarctic ice sheet exceed losses *J. Glaciol.* **61** 1019–36